Constitutive Signaling of the Human Cytomegalovirus-encoded Receptor UL33 Differs from That of Its Rat Cytomegalovirus Homolog R33 by Promiscuous Activation of G Proteins of the G_q, G_i, and G_s Classes*

Paola Casarosa,[a,b,c] **Yvonne K. Gruijthuijsen,**[b,d,e] **Detlef Michel,**[f] **Patrick S. Beisser,**[d] **Jens Holl,**[f] **Carlos P. Fitzsimons,**[a] **Dennis Verzijl,**[a,e] **Cathrien A. Bruggeman,**[d] **Thomas Mertens,**[f,g] **Rob Leurs,**[a] **Cornelis Vink,**[d,h] **and Martine J. Smit**[a,h,i]

From the [a]Leiden/Amsterdam Center for Drug Research, Division of Medicinal Chemistry, Faculty of Chemistry, De Boelelaan 1083, 1081 HV Amsterdam, The Netherlands, the [d]Department of Medical Microbiology, Cardiovascular Research Institute Maastricht, University of Maastricht, P. O. Box 5800, 6202 AZ Maastricht, The Netherlands, and the [f]Department of Virology, Institute of Microbiology, University of Ulm, Albert Einstein Allee 11, 89081 Ulm, Germany

The human cytomegalovirus (HCMV) *UL33* gene is conserved among all β-herpesviruses and encodes a protein that shows sequence similarity with chemokine receptors belonging to the family of G protein-coupled receptors. Here, we show that HCMV *UL33* is predominantly transcribed as a spliced mRNA of which the 5′ terminus is localized 55 bp upstream of the start codon. Like its homolog from rat cytomegalovirus (RCMV), R33, UL33 activates multiple signaling pathways in a ligand-independent manner. Although both receptors constitutively activate phospholipase C via $G_{q/11}$, and partially via $G_{i/o}$-mediated pathways, they exhibit profound differences in the modulation of cAMP-responsive element (CRE) activation. R33 constitutively inhibits, whereas UL33 constitutively enhances CRE-mediated transcription. For R33, the inhibition of CRE-driven transcription is entirely $G_{i/o}$-mediated. For UL33, however, CRE-mediated transcription is modulated not only through coupling to $G\alpha_{i/o}$ but also through coupling to $G\alpha_s$. In addition, UL33 was found to enhance CRE activation through the Rho/p38 pathway, via $G\beta\gamma$. Interestingly, by studying chimeric UL33/R33 proteins, we found the C-terminal cytoplasmic tail of UL33, but not that of R33, to be responsible for the activation of $G_{i/o}$ proteins. A *UL33*-deficient variant of HCMV was generated to analyze UL33-signaling properties in a physiologically relevant model system. Data obtained with infected cells show that HCMV induces CRE activation, and this effect is, at least in part, dependent on UL33 expression. Taken together, our data indicate that constitutive signaling of UL33 differs from that of R33 by promiscuous activation of G proteins of the G_q, $G_{i/o}$, as well as G_s class. Thus, HCMV may effectively use UL33 to orchestrate multiple signaling networks within infected cells.

A large number of viruses appear to have pirated genes encoding key regulatory cellular proteins (1). It is likely that these genes play important roles in strategies that are aimed at the subversion of antiviral challenges by the immune system of the viral host. One of the most prominent examples of such strategies is employed by representatives from the β- and γ-herpesvirus subfamilies. Sequence analysis of the genomes of human cytomegalovirus (HCMV),[1] Kaposi's sarcoma-associated herpes virus (KSHV), and human herpesvirus 6 and 7 (HHV-6 and HHV-7) revealed the existence of genes encoding proteins with high homology to chemokine receptors, belonging to the family of G protein-coupled receptors (GPCRs) (reviewed in Ref. 2). Because GPCRs play a crucial role in cellular communication, and chemokine receptors in particular are essential for leukocyte trafficking, the virus-encoded GPCRs (vGPCRs) may be crucial determinants of viral pathogenesis. Expression of vGPCRs may play a prominent role in immune evasion, promote virus dissemination, or modulate cellular responses of infected cells.

The β-herpesvirus HCMV can cause life-threatening systemic infections in immunocompromised individuals and has also been recognized as a risk factor for vascular diseases, like arterial restenosis and atherosclerosis (3). Within the HCMV genome, four genes encoding GPCRs have previously been identified (*US27*, *US28*, *UL33*, and *UL78*) (4). Recently, it has been suggested that the HCMV genome may contain additional putative GPCR genes (5). The US28-encoded receptor has been characterized most extensively and was shown to bind CC chemokines and the CX_3C chemokine fractalkine (6, 7). In addition, we and others have recently shown that US28 signals in a constitutive manner in both transfected and HCMV-infected cells (8–10), suggesting a physiological relevance of this property.

---

[1] The abbreviations used are: HCMV, human cytomegalovirus; KSHV, Kaposi's sarcoma-associated herpes virus; HHV, human herpesvirus; GPCR, G protein-coupled receptor; vGPCR, virus-encoded GPCR; CMV, cytomegalovirus; RCMV, rat CMV; MCMV, mouse CMV; ORF, open reading frame; EGFP, enhanced green fluorescence protein; PTX, pertussis toxin; HEL, human embryo lung fibroblast; RACE, rapid amplification of cDNA ends; BAC, bacterial artificial chromosome, HFF, human foreskin fibroblast; m.o.i., multiplicity of infection; CRE, cAMP-responsive element; TFR, transferrin receptor; InsP, inositol phosphate; PKA, protein kinase A; PKC, protein kinase C; PMA, phorbol 12-myristate 13-acetate; MAPK, mitogen-activate protein kinase; JNK, c-Jun N-terminal kinase; MEK, MAPK/extracellular signal-regulated kinase kinase; PLC, phospholipase C; RLU, relative light unit.

For the other three HCMV-encoded GPCR-like genes, little information is available. The *UL33* gene has homologs in all β-herpesviruses, including rat CMV (RCMV) *R33*, murine CMV (MCMV) *M33*, and the *U12* genes of HHV-6A, HHV-6B, and HHV-7, which may illustrate the biological significance of this gene family (reviewed in Ref. 11). The *UL33*, *M33*, and *R33* genes were found to be dispensable for viral growth *in vitro* (12–14). However, the biological significance of the UL33 family members has been demonstrated in studies *in vivo*. Recombinant RCMV and MCMV strains lacking a functional *R33* or *M33* gene, respectively, are unable to replicate in the salivary glands and induce a lower mortality in infected animals (13, 14). These results underline the importance of the *UL33*-like genes in the pathogenesis of infection.

On the basis of sequence alignments, it was suggested that the *UL33* gene family members of MCMV, HCMV, HHV-6, and HHV-7 may express spliced mRNAs (13). Indeed, transcripts of *M33*, *UL33*, as well as HHV-6B *U12* were demonstrated to be spliced (13, 15), although a previous report suggested that transcripts of *UL33* were not spliced (12). The RCMV *R33* gene, on the other hand, was found to be transcribed into an unspliced mRNA (14).

We have previously demonstrated that the RCMV *R33* gene, like *US28*, encodes a constitutively active receptor, modulating multiple signaling pathways (16). Also, the MCMV and HCMV homologs of R33, M33, and UL33, respectively, were shown to display constitutive activity (17). However, a detailed analysis of the signaling pathways underlying the observed constitutive activity displayed by UL33 has not been performed. As yet, no chemokines were reported to bind or modulate the activity of UL33, R33, or M33 (16, 17). Therefore, these proteins should be regarded as orphan receptors.

In this study, we compared the pharmacological behavior of the HCMV-encoded UL33 with that of its RCMV homolog R33. Because only limited information is available on the *UL33* gene and protein, transcriptional analysis was performed in HCMV-infected cells, and signaling pathways activated by UL33 have been extensively delineated. Like other vGPCRs, UL33 shows a considerable level of constitutive activity and couples to a wide variety of G proteins. Surprisingly, UL33 and R33 differentially modulate signaling, which was further addressed by studying UL33/R33 chimeras. Moreover, to analyze the signaling properties of the UL33 protein in HCMV-infected cells, a *UL33*-deficient variant of HCMV was generated and characterized.

MATERIALS AND METHODS

DNA Constructs—Plasmid pcDNA3/*UL33(s)* (gift from Dr. B. Margulies), contains the partial coding sequence of the HCMV strain AD169 *UL33* gene (corresponding to position 43,253–44,425 of the HCMV AD169 genome sequence, GenBank™ data base accession number NC-001347) (12). Within plasmid pcDNA3/UL33(s), the *UL33* open reading frame (ORF) starts with an ATG codon downstream of the *UL33* intron. Thus, this plasmid encodes a short (s) version of UL33, which is truncated at its N terminus. The expression vector pcDNA3/UL33, which contains the full-length coding UL33 cDNA sequence (13), was generated as follows. First, PCR amplification was performed of the *UL33* 5′ coding region (corresponding to positions 43,066–43,089 and 43,211–43,394 of the HCMV AD169 genome) using HCMV AD169 cDNA as template and primers 5′-caggatcc**tggtgggcgtcg**-3′ (the sequence in bold type is complementary to the sequence corresponding to position 43,377–43,394 of the HCMV genome; the underlined sequence indicates the position of the BamHI site) and 5′-gaggta**ccacgatggacac-catc**-3′ (the sequence in bold type corresponds to position 43,061–43,077 of the HCMV genome; the underlined sequence indicates the position of the Asp718 site). The resulting 220-bp PCR product was then digested with BamHI and Asp718, and subsequently used to replace the BamHI-Asp718 fragment containing the 5′ coding region of *UL33(s)* in plasmid pcDNA3-*UL33(s)*, thus resulting in expression vector pcDNA3/*UL33*.

To enable subsequent C-terminal tagging of the *UL33* and *UL33(s)* gene products with enhanced green fluorescent protein (EGFP), a PCR-based procedure was used to modify the sequence surrounding the stop codons of UL33 and UL33(s). Using this procedure, the sequence 5′-GTA*TGA*GCT-3′ (corresponding to position 44,420–44,428 of the HCMV genome), in which the sequence in italics represents the *UL33* and *UL33(s)* stop codons, was changed into the sequence 5′-GT-*GCTAGC*G-3′, in which the stop codon is disrupted and a unique NheI restriction site (in italics) is introduced. Subsequently, the 768-bp NheI-XbaI fragment from plasmid p368, which contains the EGFP ORF (16), was cloned in-frame into the introduced NheI sites at the 3′-end of the *UL33* and *UL33(s)* ORFs, generating expression vectors pcDNA3/UL33-EGFP and pcDNA3/UL33(s)-EGFP, respectively.

A PCR-based procedure was used to generate vectors pcDNA3/R33-R-UL33, pcDNA3/R33-Y-UL33, pcDNA3/UL33-R-R33, and pcDNA3/UL33-Y-R33, which express pR33/pUL33 chimeric proteins as schematically depicted below in Fig. 3. The vectors pcDNA3/R33-Y-UL33-EGFP, pcDNA3/R33-R-UL33-EGFP, pcDNA3/UL33-Y-R33, and pcDNA3/UL33-R-R33-EGFP, expressing the respective chimeric receptors with a C-terminal EGFP tag, were generated in a similar fashion as described above for the UL33 expression constructs. The integrity of all DNA constructs was verified by sequence analysis. The expression vectors pcDNA3/EGFP, pcDNA3/R33, and pcDNA3/R33-EGFP have been described previously (16). The reporter plasmid pTLNC-21CRE was obtained from W. Born (National Jewish Medical and Research Center, Denver, CO). Gifts of pcDNA3-based expression vectors containing the cDNAs of $G\alpha_q$ (Dr. B. Conklin), $G\alpha_{11}$ and $G\alpha_{11}$* (Q209L, Dr. H. Umemori), $G\alpha_s$ and $G\alpha_s$* (R201E, Dr. R. Iyengar), $G\alpha_{16}$ (Dr. S. Rees), $G\alpha_{12}$ and $G\alpha_{13}$ (Dr. N. Dhanasekaran), $G\alpha_t$ (Dr. H. Bourne), PTX-insensitive (C351/2G) $G\alpha_o$, $G\alpha_{i1}$, $G\alpha_{i2}$, and $G\alpha_{i3}$ mutants (Dr. G. Milligan), the C3 exoenzyme (Dr. S. Narumiya), and GRK2-K220R (Dr. S. Cotecchia) are gratefully acknowledged.

Cell Culture and Transfection—COS-7 cells were grown and transfected as previously described (8). The astrocytoma cell line U373 was grown in Dulbecco's modified Eagle's medium supplemented with 10% fetal calf serum.

Determination of cDNA Ends—Propagation of human embryo lung fibroblasts (HEL) and HCMV AD169 was performed as previously described (18, 19). HEL were infected with HCMV AD169 at a multiplicity of infection (m.o.i.) of 0.1 as described earlier (18). At 72 h postinfection, infected as well as uninfected HEL were detached from culture flasks by using a cell scraper. Approximately 10^7 cells per sample were subjected to poly(A)$^+$ RNA extraction by using a QuickPrep Micro mRNA purification kit (Amersham Biosciences, Roosendaal, The Netherlands) according to the manufacturer's protocol. Subsequently, 1-μg portions were used for cDNA synthesis and PCR using a SMART™ RACE cDNA amplification kit (Clontech/Westburg, Leusden, The Netherlands) according to the manufacturer's protocol. For the amplification of UL33-specific cDNA, a gene-specific primer with the sequence 5′-AAGCGGT-TGTGGCATAACTGTTGAAGATCA-3′ (complementary to GenBank™ accession NC-001347, bases 43,976–44,424) was included in the reaction. The PCR reaction mixtures were incubated in a GeneAmp Systems 9600 thermal cycler (PerkinElmer Life Sciences, Nieuwerkerk aan de IJssel, The Netherlands) with the following settings: 5 cycles of 5 s at 94 °C, and 3 min at 72 °C, 5 cycles of 5 s at 94 °C, 10 s at 70 °C, and 3 min at 72 °C, and 22 cycles of 5 s at 94 °C, 10 s at 68 °C, and 3 min at 72 °C. Subsequent to the incubation, 5-μl samples from each of the PCR mixtures was analyzed by agarose gel electrophoresis and ethidium bromide staining. In addition, a 1-μl sample from the *UL33*-specific PCR mix was used for cloning of the PCR product into vector pGEM®-T Easy (Promega Benelux BV, Leiden, The Netherlands). The resulting plasmids were transformed in *Escherichia coli* TOP10 cells. Plasmids from several *E. coli* colonies were sequenced by using a Thermo Sequenase cycle sequence kit (Amersham Biosciences) and standard M13 forward and reverse sequencing primers. Finally, the sequences were compared with sequences from the non-redundant nucleotide sequence data base at the National Center for Biotechnology Information (NCBI, Bethesda, MD) using the Basic Local Alignment Search Tool (20).

Confocal Imaging—Transiently transfected COS-7 cells were grown on glass coverslips. After 48 h, the cells were fixed for 10 min with 3.7% formol in phosphate-buffered saline, and the coverslips were mounted for subsequent confocal imaging. Confocal images were collected at a wavelength of 488 nm and processed as described previously (16).

Reporter Gene Assay—COS-7 cells transiently co-transfected with the reporter plasmid pTLNC-21CRE (containing 21 cAMP-responsive elements upstream of the luciferase cDNA) and either pcDNA3 (mock) or any of the expression constructs were seeded in 96-well white plates in serum-free culture medium in the presence or absence of PTX (80

ng/ml). After 24 h, selected samples were stimulated with forskolin (1 μM) for a period of 6 h. Incubation was stopped by aspiration of the medium, and cells were assayed for luminescence as described previously. Luminescence was measured for 3 s in a Wallac Victor[2] multilabel plate reader (PerkinElmer Life Sciences, Boston, MA).

[³H]Inositol Phosphate Production—Experiments in COS-7 cells were performed as previously described (8).

BAC Mutagenesis—Recombinant *UL33*-deficient HCMV genome was generated in *E. coli* using a recently established new method that relies on homologous recombination of a linear PCR fragment with the HCMV BAC plasmid (21–23). The PCR product was generated with the primer pair prim5′-*UL33* 5′-CCG CCC AGA CCC GCA ACA ACA CTC CTC CGC ACA TCA ATG ACA CTT GCA ACC GTC GTG GAA TGC CTT CGA ATT C-3′ and prim3′-UL33 5′-GGG AAA TGG CGA CGG GTT CTG GTG CTT TCT GAA TAA AGT AAC AGG AAA GCA CAA GGA CGA CGA CGA CAA GTA A-3′ (sequences homologous to the pSL-FRTKn plasmid are underlined). The amplicon contained homologies of ~50 bp upstream or downstream of the positions of the deleted *UL33* ORF using the plasmid pSLFRTKn (21–23) (kindly provided by Dr. M. Wagner, Munich) as template DNA. After purification and DpnI digestion (21) this PCR fragment was inserted into pHB5 (23) by homologous recombination in *E. coli*, which was mediated by the recombination plasmid pKD46 leading to deletion of the native UL33 start and stop codons and the insertion of a kanamycin cassette that is flanked by Flp recombination target sites. The kanamycin gene was excised via the flanking Flp recombination target sites by Flp-mediated recombination as described previously (21, 22, 23) generating the HCMV BAC plasmid pUL33del. BAC DNA *pUL33del* was isolated from *E. coli* cultures with an alkaline lysis procedure (24) and purified with NucleoBond PC 500 columns (Macherey-Nagel, Düren, Germany). Correct mutagenesis was confirmed by PCR analysis using the primer pair *UL33*ATG, 5′-CGC ACA TCA ATG ACA CTT GC-3′ and UL33TGA 5′-TGA ATA AAG TAA CAG GAA AGC-3′.

Reconstitution of UL33-deficient HCMV—Mutant viruses were reconstituted by transfection of BAC DNA pUL33del into human foreskin fibroblasts (HFF) with the SuperFect transfection reagent (Qiagen, Hilden, Germany) according to the manufacturer's instructions. Briefly, 5 μg of BAC DNA was incubated with 150 μl of medium without serum and 30 μl of SuperFect transfection reagent. The mixture was added to ~3 × 10⁵ HFF cells. Cells were washed with phosphate-buffered saline 2 h later, cultured with fresh medium. Cells were passaged 7 days after transfection. Infectious supernatants were harvested when 100% of cells showed cytopathic effects. Virus stocks were prepared on HFF. All virus titers were determined by standard assays. DNA of reconstituted virus mutants was analyzed in parallel by Southern blotting and PCR to prove the correct deletions of the UL33 gene.

Viral Nucleic Acid Isolation and Analysis—Fibroblasts were infected at an m.o.i. of 1, harvested 3 days post infection when cultures reached 100% cytopathic effect, and collected by centrifugation. Cells were lysed in a solution containing 50 mM Tris-HCl (pH 8.0), 10 mM EDTA, and 0.5% SDS. Proteinase K digestion (500 μg/ml) was performed for 3 h at 56 °C. Total DNA was extracted with phenol-chloroform and precipitated with isopropanol. Southern blot analysis was performed as described previously (25).

CRE Activation in HCMV-infected Cells—U373 cells were plated in six-well plates (~250,000 cells/well) and transiently transfected with the reporter gene pTLNC-21CRE with the calcium phosphate method. 16 h later, cells were infected with HCMV (strain AD169) or AD169-ΔUL33 at an m.o.i. of 3. At different time points after infection, cells were lysed and assayed for luciferase activity (8).

Data Analysis—Data were analyzed using the program Prism (GraphPad Software, Inc., San Diego, CA). Data are expressed as mean ± S.E.

RESULTS

Transcriptional Analysis of UL33 in HCMV-infected Cells—Although HCMV *UL33* was originally thought to express an unspliced mRNA (12), Davis-Poynter and coworkers demonstrated that *UL33* is transcribed as a spliced mRNA (13) (Fig. 1*A*). As a consequence, the *UL33* gene encodes a protein that is 22 amino acids longer than the protein that was previously predicted to be encoded by *UL33* (12). Nevertheless, it has not yet been established whether *UL33* can also be transcribed into unspliced mRNAs, potentially coding for alternative protein products. To investigate this possibility, fibroblasts were infected with HCMV AD169. After purification of mRNA from the

cells, the 5′ termini of the *UL33* transcripts were assessed by rapid amplification of cDNA ends (RACE). First, the integrity of the cDNA samples was checked by using primers specific for the human transferrin receptor (TFR). As expected, the TFR-control 5′-RACE reaction produced a major DNA fragment of 2.3 kb (Fig. 1*B*, *lane 1*). Subsequently, a 5′-RACE reaction was performed using the *UL33*-specific antisense primer. This reaction resulted in the amplification of a major DNA species with a length of 0.9 kb (Fig. 1*B*, *lane 2*). Several minor, smaller fragments were also observed in this sample. To determine the sequence of these fragments, a portion of the 5′-RACE sample was used for subcloning into a sequencing vector. Plasmids purified from 15 independent bacterial colonies were sequenced. The resulting sequences were compared with those of the GenBank™ nucleotide sequence data base. This comparison indicated that all 15 clones contained *UL33*-specific sequences. The length of the insert in 8 out of 15 clones corresponded to that of the major, 0.9-kb PCR product in Fig. 1*B* (*lane 2*). Each of these inserts was found to be the product of splicing, similarly as described previously (13). Out of these eight clones, seven were found to have the same 5′ cDNA end. This end was localized 55 bp upstream of the *UL33* start codon (Fig. 1*C*), whereas one of these eight terminated at 31 bp upstream of the first start codon (Fig. 1*C*). The inserts from the other seven out of 15 clones were likely derived from the minor PCR products seen in Fig. 1*B* (*lane 2*), because these were all smaller than 0.9 kb. The 5′ cDNA ends of two of these clones were at 22 and 3 bp, respectively, upstream of the "second" *UL33* ATG codon, localized downstream of the intron sequence (Fig. 1*C*). The 5′ cDNA termini of the other five clones were at significantly larger distances downstream from the second ATG codon (at 140, 200, 258, 259, and 283 bp, respectively). The differences in structure of the last seven cDNA clones suggest that the corresponding cDNA fragments were the result of amplification of either truncated transcripts or truncated first-strand cDNA species. Given the relative abundance of the 0.9-kb 5′-RACE product, which constitutes ~85% of the total population of amplified products (Fig. 1*B*, *lane 2*), we conclude that HCMV *UL33* predominantly encodes a spliced transcript of which the 5′ terminus is localized 55 bp upstream of the start codon within *UL33* exon 1. Because cDNA corresponding to unspliced *UL33* transcripts were not detected, we conclude that such mRNA species do not play a role in HCMV infection. For completeness of the study, however, a plasmid containing the cDNA corresponding to the unspliced *UL33* ORF variant, designated UL33(s), was included in the signal transduction assays.

Expression of and Constitutive Signaling by UL33, UL33(s), and R33—To investigate the signaling properties of UL33, we transfected COS-7 cells with cDNAs coding for full-length *UL33* and for the unspliced, shorter variant, *UL33(s)*, which lacks the N-terminal 22 amino acids. The RCMV homolog of UL33, R33, previously found to display constitutive activity (16), was used in the different assays for comparison.

Transfection of increasing amounts of DNA encoding UL33 in COS-7 cells was accompanied by an agonist-independent increase in [³H]inositol phosphates (InsPs) production, comparable to that observed for R33 (Fig. 2*A*). In contrast to the observed constitutive activity displayed by UL33, UL33(s) did not induce an increase in InsP production upon transfection of either 2 μg (Fig. 2*A*) or 5 μg (data not shown) cDNA. To monitor the expression of *UL33* and *UL33(s)*, both proteins were tagged C-terminally with EGFP. These proteins, UL33-EGFP and UL33(s)-EGFP, displayed similar signaling activities as their native counterparts (data not shown). Their expression, as well as that of EGFP and R33-EGFP, was studied by confocal mi-
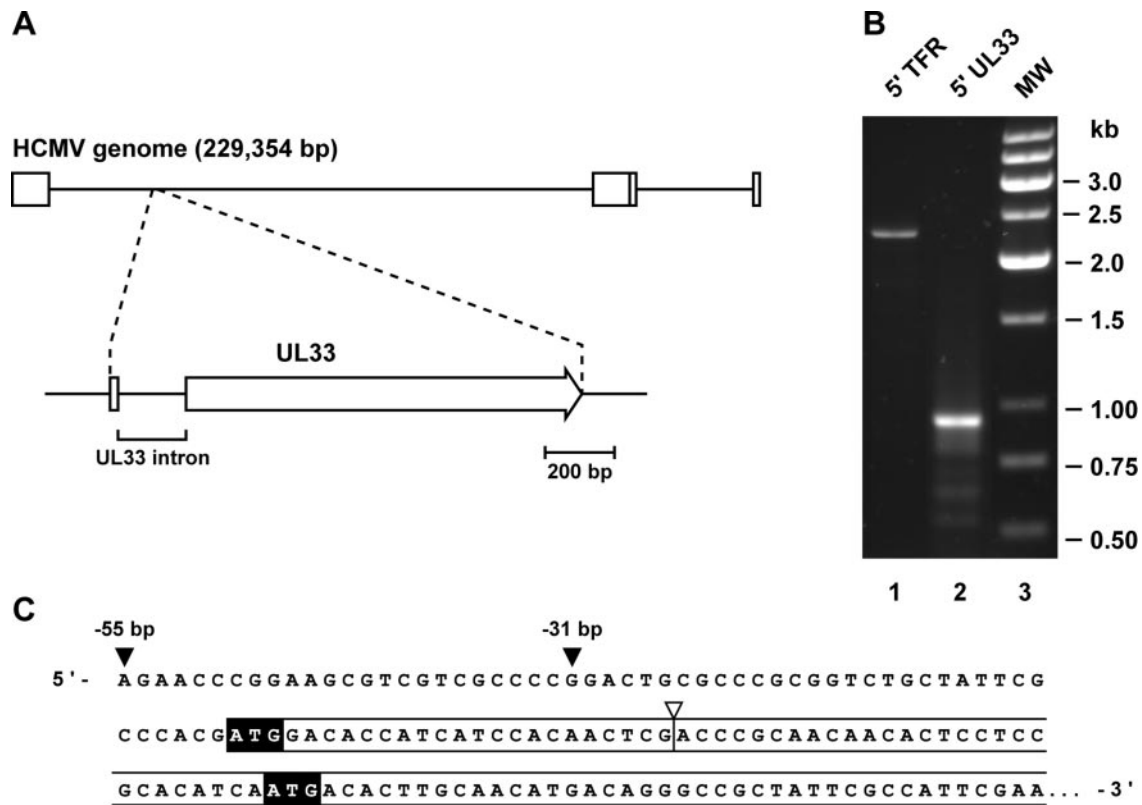
FIG. 1. **The structure of the 5′-ends of HCMV *UL33* transcripts.** *A*, the position of the *UL33* locus on the HCMV genome. The HCMV genome is indicated by a *horizontal black line*. Genomic repeat regions are indicated by *white boxes*. The *UL33* gene is superimposed below the indicated genome. Here, the coding region of *UL33* is indicated by a *white box* (coding region within exon 1) and a *white arrow* (coding region within exon 2). The *arrow* indicates the polarity of *UL33*. *B*, rapid amplification of HCMV *UL33*-specific and human transferrin receptor (*TFR*)-specific cDNA ends (RACE). The figure shows an ethidium bromide-stained agarose gel containing 5′-TFR-specific (*lane 1*) and 5′-UL33-specific reaction mixtures (*lane 2*). The sizes of the molecular weight marker bands (*lane 3*) are indicated at the *right-hand side* of the agarose gel in kb. *C*, the 5′ cDNA sequence of RACE-derived UL33-specific fragments. The UL33 coding sequence is enclosed in a *white box*. The *UL33* start codon, as well as a second, downstream ATG codon, are enclosed in *black boxes*. The *black arrowheads* indicate the positions of the first bases found in the 5′-untranslated region of the UL33-specific RACE fragments. The *white arrowhead* indicates the junction where the UL33 intron has been excised.

croscopy of transfected cells. Fig. 3*A* shows that the fluorescence within cells expressing native EGFP is seen dispersed throughout the nucleus and cytoplasm. However, in cells expressing either UL33-EGFP or R33-EGFP, the fluorescent signal clearly co-localized with the cell membrane as well as with intracellular, perinuclear vesicles (Fig. 3, *B* and *C*). This indicates that UL33-EGFP, like R33-EGFP, is properly expressed on the cell surface of transfected cells. By contrast, the fluorescence in cells expressing UL33(s)-EGFP did not co-localize with the cell membrane, and seemed to be confined to intracellular compartments (Fig. 3*D*). This observation shows that UL33(s)-EGFP is retained intracellularly and thus explains the observed lack of constitutive signaling for UL33(s).

UL33-mediated Inositol Phosphate Accumulation Is a $G_{q/11}$- and Partially $G_{i/o}$-dependent Process—Accumulation of InsP can be achieved following activation of phospholipase C by $G\alpha$ subunits of the $G_{q/11}$ family as well as by $G\beta\gamma$ subunits (26). Previously, we have shown that the R33-mediated increase in InsP accumulation is partially mediated by the $G\beta\gamma$ subunits of activated $G_{i/o}$ proteins (16). Also for UL33, the observed increase of InsP accumulation can be partially attributed to involvement of $G_{i/o}$ proteins. Incubation of cells expressing UL33 with pertussis toxin (PTX) (24 h, 80 ng/ml) led to a $40 \pm 5\%$ ($n = 6$) decrease of InsP production (Fig. 2, *A* and *B*). Co-expression of UL33 and $G\alpha_t$, known to sequester $G\beta\gamma$ subunits, resulted in a $43 \pm 6\%$ ($n = 2$) attenuation of InsP production, similar to that observed for PTX treatment (Fig. 2*B*). PTX treatment did not further abrogate the InsP production in cells co-expressing UL33 and $G\alpha_t$, suggesting that $G\beta\gamma$ subunits

from $G_{i/o}$ are in part responsible for the observed increase in InsP production.

The remaining increase in InsP production may be ascribed to the involvement of $G\alpha$ proteins of in particular the $G_{q/11}$ family. Co-expression of UL33 with either $G\alpha_q$ or $G\alpha_{11}$ proteins enhanced the UL33-mediated production of [³H]InsP ($196 \pm 14\%$ and $144 \pm 4\%$ of UL33 basal signaling, respectively, $n = 3$; Fig. 2*C*). The contribution of both $G\alpha_{q/11}$ as well as $G\beta\gamma$ subunits of the $G_{i/o}$ family in the UL33-mediated accumulation of InsP production was further corroborated by use of the kinase-deficient GRK2-K220R mutant (27). This mutant has been reported to scavenge both $G\alpha_{q/11}$ via interaction with its RGS domain and $G\beta\gamma$ subunits via binding to its pleckstrin homology domain (27). As anticipated, co-expression of the kinase-deficient GRK2K220R mutant resulted in a complete inhibition of UL33-mediated InsP production ($n = 3$; Fig. 2*B*).

G Proteins Involved in UL33-mediated Constitutive Modulation of CRE—Although R33 and UL33 both constitutively activate phospholipase C, these receptors differentially regulate CRE-mediated transcription. Expression of UL33 resulted in a concentration-dependent increase in CRE-mediated transcription (Fig. 4*A*). As expected, UL33(s) did not modulate CRE activity. R33, however, inhibited the forskolin-induced CRE transcription in a concentration-dependent fashion (Fig. 4*B*). Because basal cAMP levels are low in COS-7 cells, forskolin, known to activate adenylyl cyclase, was used to allow detection of inhibitory signaling to CRE (28). This decrease in R33-mediated CRE activation can be ascribed to involvement of $G_{i/o}$ proteins, because PTX markedly reversed the R33-induced in-
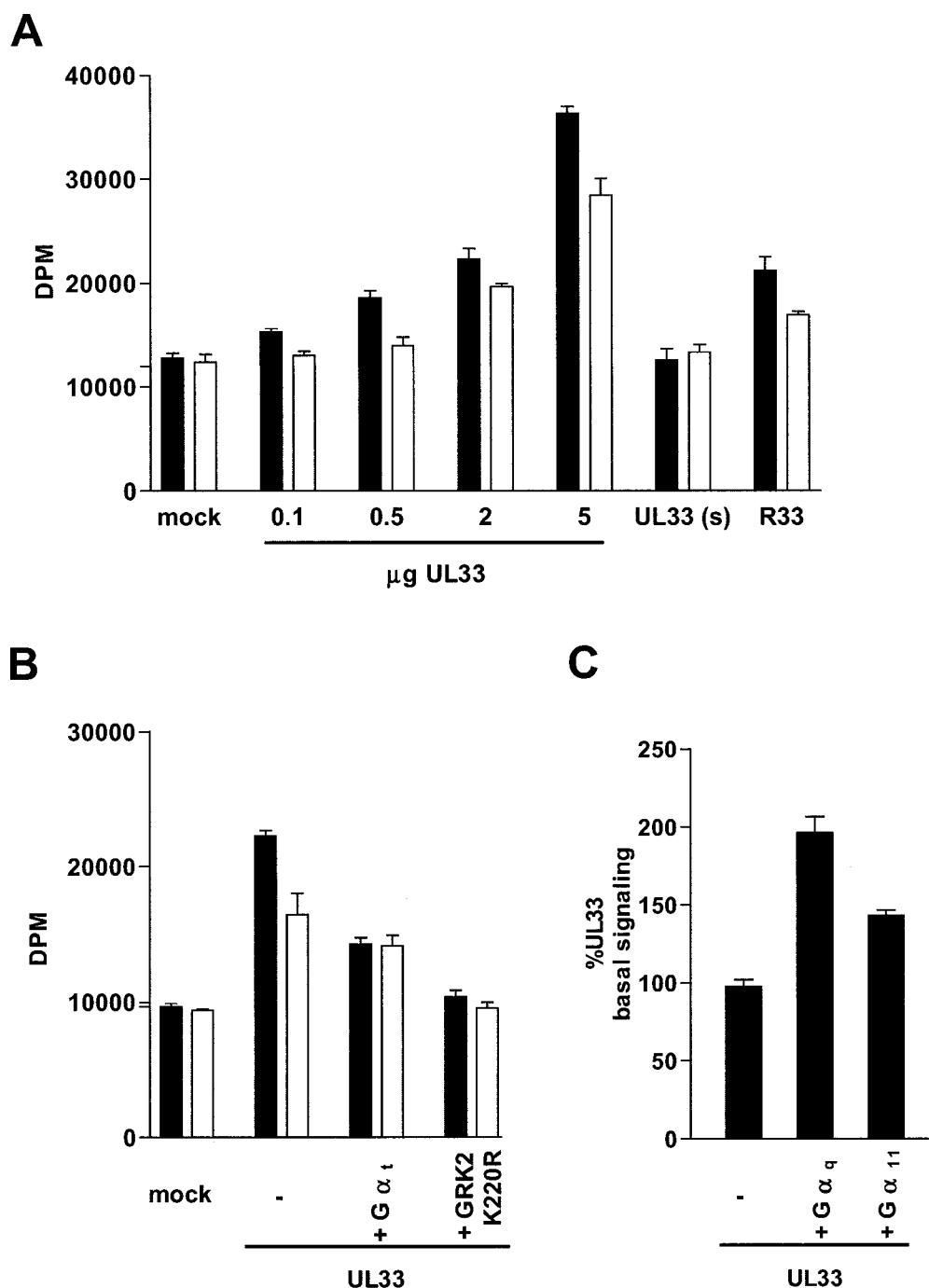
Differential Signaling by CMV-encoded Receptors UL33 and R33

FIG. 2. **UL33 and R33 induction of inositol phosphate accumulation.** *A*, COS-7 cells (1×10^6 cells) were transiently transfected with increasing amounts of cDNA encoding UL33, 2 μg of UL33(s), and 2 μg of R33. Cells were incubated in the presence (*white bars*) or absence (*black bars*) of PTX (80 ng/ml). 48 h after transfection InsP accumulation was measured. *B*, COS-7 cells were transiently transfected with empty vector (mock) or UL33 (1 μg/10^6 cells) in the presence of either Gα transducin or the kinase-deficient GRK2-K220R (1 μg/10^6 cells). Cells were incubated in the presence (*white bars*) or absence (*black bars*) of PTX (80 ng/ml). 48 h after transfection InsP accumulation was measured. *C*, COS-7 cells were transiently transfected with UL33 (1 μg/10^6 cells) together with cDNAs encoding Gα_q or Gα_{11} subunits (1 μg/10^6 cells); 48 h after transfection InsP accumulation was measured. Data are presented as percentages of UL33-mediated response, defined as absolute increase of UL33-mediated InsP accumulation above values obtained for mock transfected cells.

hibition of forskolin-mediated CRE transcription. Interestingly, inactivation of G$_{i/o}$ by PTX in UL33-expressing cells led to a potentiation of the basal increase in CRE transcription (Fig. 4*A*), indicating that the UL33-mediated stimulation of CRE transcription is the result of the activation of both inhibitory and stimulatory pathways that converge at the level of CRE. The observed inhibition of UL33-mediated signaling to CRE can be attributed to coupling of the receptor to either Gα_{i1}

or Gα_{i3}, as co-expression of the respective subunits resulted in a complete inhibition of UL33-induced signaling (Fig. 5*A*). Co-expression of Gα_o or Gα_{i2} had no effect on UL33-mediated signaling, suggesting selectivity of coupling for UL33 within this class of proteins. All used G$_{i/o}$ constructs are PTX-insensitive (via a mutation of Cys$^{351/2}$ to Gly), and consequently, no increase was observed upon PTX treatment for Gα_{i1} or Gα_{i3}. Similarly, R33 showed preferential coupling to Gα_{i1} and Gα_{i3}
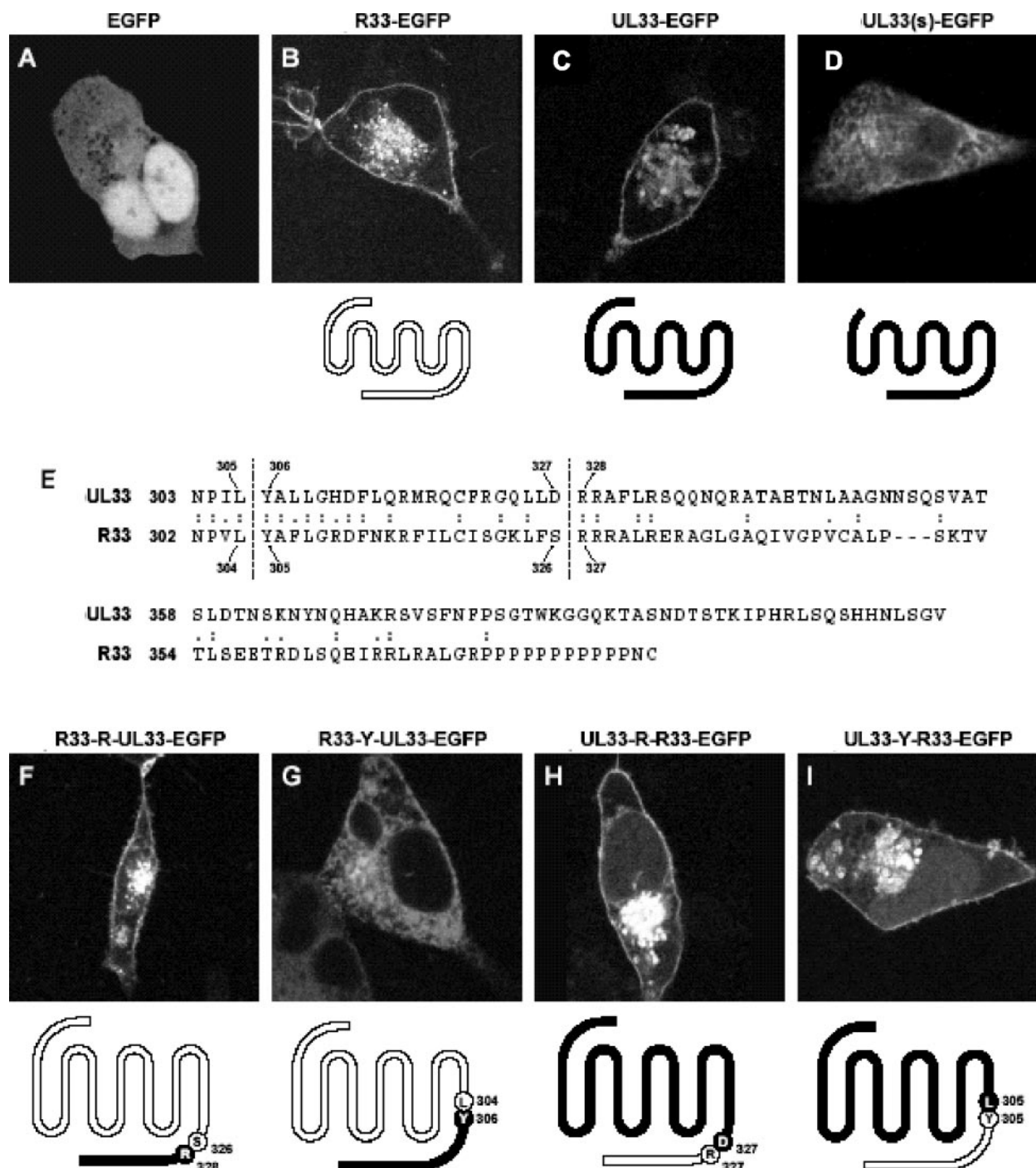
FIG. 3. **Expression of R33, UL33, and UL33/R33 chimeras.** *A–D*, confocal images of cells expressing EGFP, R33-EGFP, UL33-EGFP, and UL33(s)-EGFP. COS-7 cells were transiently transfected with either pcDNA3/EGFP (*A*), pcDNA3/R33-EGFP (*B*), pcDNA3/UL33-EGFP (*C*), or pcDNA3/UL33(s)-EGFP (*D*) (2 μg/10[6] cells), fixed after 48 h and subjected to confocal microscopy at 488 nm. *E*, alignment of the C-terminal portions of UL33 and R33 amino acid sequences. Identical residues are indicated by ":", similar residues are indicated by ".", and a *dashed vertical line* indicates the position where a UL33/R33 or R33/UL33 junction was created to generate the chimeric receptors. *F–I*, confocal images of cells expressing EGFP-tagged, UL33/R33 chimeras. COS-7 cells were transiently transfected with either pcDNA3/R33-R-UL33-EGFP (*F*), pcDNA3/R33-Y-UL33-EGFP (*G*), pcDNA3/UL33-R-R33-EGFP (*H*), and pcDNA3/UL33-Y-R33-EGFP (*I*) (2 μg/10[6] cells). A schematic representation of the amino acid sequence of each receptor is given below the respective confocal images. Sequences derived from UL33 are depicted in *black*, and R33-derived sequences are depicted in *white*. Residues flanking UL33/R33 or R33/UL33 junctions are depicted as *encircled letters* accompanied by the number corresponding to their position in the original amino acid sequence of UL33 or R33 (see *E*).

(Fig. 6*A*). All $G\alpha_{i/o}$ subunits were previously shown to be properly expressed and able to signal in the presence of the adenosine A_1 receptor (29) or the histamine H_3 receptor.[2]

To understand which other G proteins might be involved in

UL33-mediated CRE activation, another panel of $G\alpha$ subunits was tested. Expression of the different $G\alpha$ subunits did not significantly alter the basal or forskolin-induced CRE transcription in mock cells (data not shown). Co-expression of $G\alpha_{16}$, $G\alpha_{12}$, and $G\alpha_{13}$, did not modulate the constitutive signaling induced by UL33 (Fig. 5*B*). On the other hand, co-expression of $G\alpha_q$, for which coupling to UL33 was already shown in the InsP
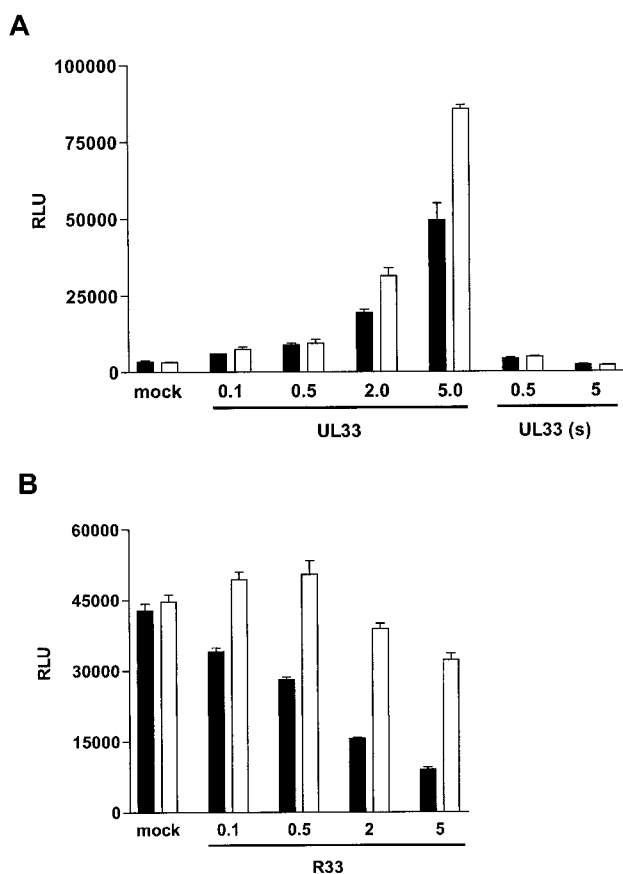
A

B

FIG. 4. **Different behavior of UL33 and R33 in CRE-mediated transcription.** *A*, COS-7 cells (1×10^6 cells) were transiently transfected with the reporter plasmid pTLNC-21CRE (containing 21 cAMP-responsive elements in front of cDNA encoding luciferase; 5 μg/10^6 cells) and increasing amounts of cDNA encoding UL33, or UL33(s). Cells were incubated in the presence (*white bars*) or absence (*black bars*) of PTX (80 ng/ml). One day after transfection, CRE-driven luciferase expression was measured. *B*, COS-7 cells were transiently transfected with pTLNC-21CRE and increasing amounts of cDNA encoding R33. Cells were incubated in the presence (*white bars*) or absence (*black bars*) of PTX (80 ng/ml). After 24 h, cells were stimulated with forskolin (1 μM) for additional 6 h, then CRE-driven luciferase expression was measured. Results are presented as relative light units (*RLUs*).

assay, decreased UL33-mediated CRE transcription (Fig. 5*B*). To investigate whether activation of Gα subunits of the q/11 class might be responsible for a negative regulation of CRE-mediated transcription, the CRE-reporter gene was co-transfected with a constitutively active Gα_{11} subunit (Gα_{11}-Q209L; Gα_{11}*). Expression of Gα_{11}* did not alter basal or forskolin-induced activation of CRE when compared with mock transfected cells (data not shown). Similarly, activation of protein kinase C (PKC) by phorbol 12-myristate 13-acetate (PMA, 300 nM) did not induce any change in the transcriptional activation of CRE (data not shown). Taken together, these data imply that activation of the G$_{q/11}$-PKC signaling pathway is not modulating CRE activation.

Interestingly, co-expression of Gα_s increased UL33-mediated signaling to CRE (204 $\pm$ 9% of UL33 basal signaling, $n = 6$, Fig. 5*B*), suggesting that UL33 coupling to Gα_s is, at least in part, responsible for CRE activation. As a control, the effect of Gα_s was monitored in R33-transfected cells. Only a minor increase in CRE activation was detected for both mock and R33-transfected cells (Fig. 6*B*), suggesting that R33, differently from UL33, is not coupling to Gα_s. The small increase in signaling in the presence of Gα_s might be due to basal activity of this α subunit or to its coupling to receptors endogenously present in COS-7 cells.
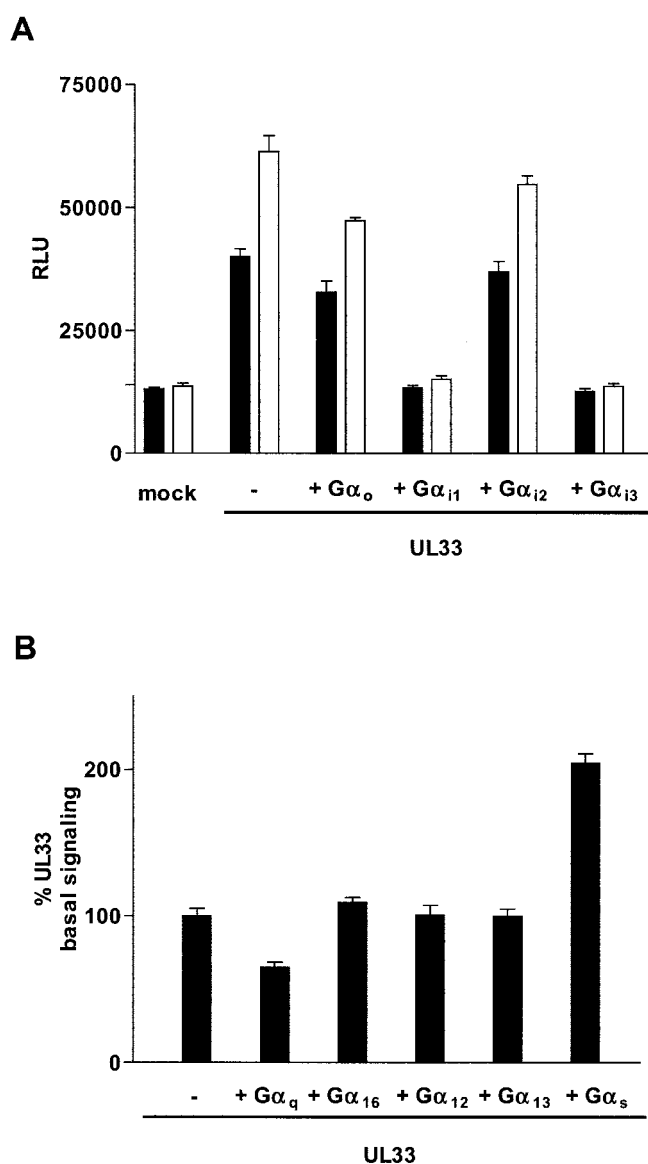
A

B

FIG. 5. **Effect of various Gα subunits on the UL33-mediated CRE activation.** *A*, COS-7 cells were transfected with pTLNC-21CRE and either pcDNA3 (mock) or UL33 (1 μg/10^6 cells), together with cDNAs encoding the indicated Gα subunits (1 μg/10^6 cells). Cells were incubated in the presence (*white bars*) or absence (*black bars*) of PTX (80 ng/ml). One day after transfection CRE-driven luciferase expression was measured. Data are presented as relative light units (*RLUs*). *B*, COS-7 cells were transfected with pTLNC-21CRE and UL33 (1 μg/10^6 cells), together with cDNAs encoding the indicated Gα subunits (1 μg/10^6 cells). One day after transfection CRE-driven luciferase expression was measured. Data are presented as percentage of UL33-mediated response, defined as absolute increase of UL33-mediated CRE transcription above values obtained for mock transfected cells.

Additional Downstream Signaling Components Involved in UL33 Signaling to CRE—CRE transcription is known to be regulated by elevation of cAMP following Gα_s activation, leading to activation of protein kinase A (PKA), which subsequently phosphorylates CREB, initiating CRE transcription (30). However, besides PKA also other signaling entities, including, *e.g.* PKC, MAPKs (p44/p42, p38, and JNK), and small G proteins, are known to regulate CRE transcription in a tissue-specific manner (30). UL33-mediated increase in CRE transcription is not mediated via p44/p42 MAPK, phosphoinositide 3-kinase, or protein kinase C signaling pathways as their respective specific inhibitors U0126 (MEK inhibitor), wortmannin (phosphoinositide 3-kinase inhibitor), and bisindolylmaleimide (PKC inhibi-
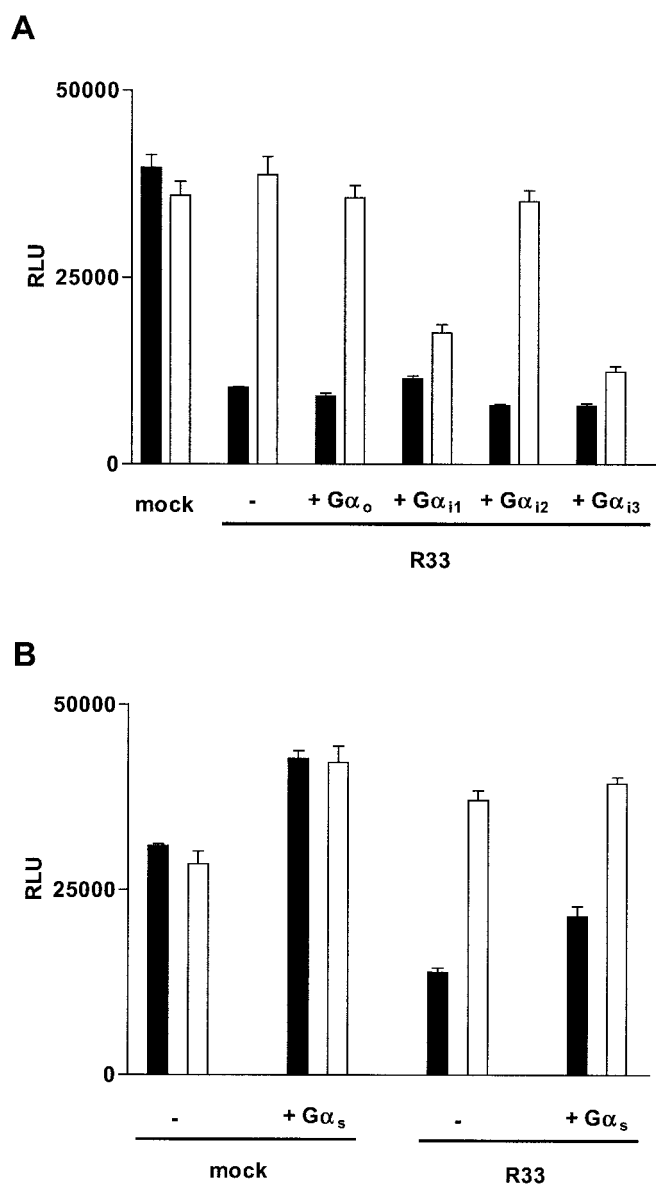
A

B

FIG. 6. **Effect of various Gα subunits on the R33-mediated CRE activation.** *A*, COS-7 cells were transfected with pTLNC-21CRE and either pcDNA3 (mock) or R33 (1 μg/10⁶ cells), together with cDNAs encoding the indicated Gα subunits (1 μg/10⁶ cells). Cells were incubated in the presence (*white bars*) or absence (*black bars*) of PTX (80 ng/ml). After 24 h, cells were stimulated with forskolin (1 μM) for additional 6 h, then CRE-driven luciferase expression was measured. Data are presented as relative light units (*RLUs*). *B*, COS-7 cells were transfected with pTLNC-21CRE and either pcDNA3 (*mock*) or R33 (1 μg/10⁶ cells), together with cDNA encoding the Gα$_s$ subunit (1 μg/10⁶ cells). Cells were incubated in the presence (*white bars*) or absence (*black bars*) of PTX (80 ng/ml). After 24 h, cells were stimulated with forskolin (1 μM) for additional 6 h, then CRE-driven luciferase expression was measured. Data are presented as relative light units (*RLUs*).

tor) did not abrogate the UL33-induced signaling to CRE (Fig. 7*A*). These inhibitors, however, do inhibit signaling of the KSHV-encoded receptor ORF74 to p44/p42 MAPK in COS-7 cells, indicating proper effectiveness (31). The specific inhibitor of p38, SB203580, on the other hand, markedly inhibited the UL33 effect (43 ± 5% inhibition of UL33 basal signaling, $n = 3$; Fig. 7*A*).

Upstream activators of p38 are, among others, small G proteins of the Rho family (32, 33). Co-expression of C3 exoenzyme, which is known to inactivate these G proteins (by ADP-ribosylation of Asn[41]) (34), resulted in a marked inhibition of UL33-induced activation of CRE transcription (40 ± 3% inhibition of

UL33 basal signaling, $n = 3$), similar to that obtained with the p38 inhibitor SB203580 (Fig. 7*B*). Co-expression of C3 exoenzyme or treatment with the p38 inhibitor SB203580 did not alter R33 signaling (data not shown). These data suggest that UL33, differently from R33, engages the Rho/p38 pathway in its signaling to CRE (Fig. 7*B*).

To examine whether the Gα$_s$ and Rho pathway are connected, we determined the effect of the C3 toxin on Gα$_s$-mediated signaling. Co-expression of C3 exoenzyme did not abrogate the increase in CRE transcription induced by expression of constitutively active Gα$_s$ (Gα$_s$R201E; Gα$_s$*), indicating that the Gα$_s$ and Rho pathways do not coincide (Fig. 7*C*).

Next, we investigated which upstream signaling components were involved in UL33-mediated activation of Rho. Gα$_{12/13}$ and Gα$_{q/11}$, known to activate Rho (35), did not play a role in the UL33-mediated increase in CRE transcription, as can be seen in Fig. 5*B*. It has previously been reported that also Gβγ subunits can activate small GTPases of the Rho family, resulting in activation of p38 (36). Consequently we determined the role of Gβγ subunits in UL33-mediated activation of CRE by co-expression of Gα$_t$. As can be seen in Fig. 7 (*B* and *C*), Gα$_t$ markedly attenuated the UL33-induced transcription of CRE (49 ± 5% inhibition of UL33 basal signaling, $n = 3$), while not affecting Gα$_s$* signaling, used as a control. Co-expression of C3 toxin and Gα$_t$ did not lead to a further decrease in UL33-mediated signaling, suggesting that Gβγ subunits, through activation of the Rho/p38 pathway, may lead to activation of CRE-mediated transcription (Fig. 7*B*).

Signaling by UL33 and R33 Chimeric Proteins—Because the C-terminal tail is an important determinant of receptor signaling in general, and UL33 and R33 exhibit marked differences in their C-tails, we constructed receptor chimeras in which their C-tails were either partially or completely exchanged (Fig. 3*E*). Exchange of the entire C-terminal tails was made at a conserved tyrosine residue at positions 306 and 305 in UL33 and R33, respectively (R33-Y-UL33 and UL33-Y-R33), and the partial exchange of the C terminus was made at a conserved arginine residue at positions 328 and 327 in UL33 and R33, respectively (R33-R-UL33 and UL33-R-R33). To confirm proper expression of the chimeric receptors, we also generated C-terminal EGFP-tagged variants of these proteins, which were studied by confocal microscopy. As shown in Fig. 3 (*F*, *H*, and *I*), the fluorescence patterns of the EGFP-tagged chimeras, R33-R-UL33-EGFP, UL33-R-R33-EGFP, and UL33-Y-R33-EGFP were similar to that seen for UL33-EGFP and R33-EGFP, showing co-localization with the cell membrane of transfected cells as well as with intracellular vesicles. However, in cells expressing R33-Y-UL33-EGFP, fluorescence was seen exclusively within intracellular compartments (Fig. 3*G*), indicating that R33-Y-UL33-EGFP is not properly delivered to the cell membrane.

Subsequently, the chimeric proteins were tested in the various signaling assays. In each of these assays, the activity of the chimeric receptors was similar to that of their EGFP-fused counterparts (data not shown). Fig. 8*A* shows that, in comparison with UL33, UL33-R-R33 is impaired in activation of G$_{i/o}$ proteins, leading to an increased basal level of CRE activation (Fig. 8*A*) as well as an impaired accumulation of InsP (Fig. 8*C*). This impairment is even more pronounced for the chimera UL33-Y-R33, which appears to be completely incapable of G$_{i/o}$ coupling. In agreement with these observations, UL33-R-R33 showed a lower sensitivity to PTX than UL33, whereas the activity of UL33-Y-R33 was not significantly influenced by PTX.

The activity of R33-R-UL33, both in the CRE reporter gene assay (Fig. 8*B*) and in the InsP assay (Fig. 8*D*), was not signif-
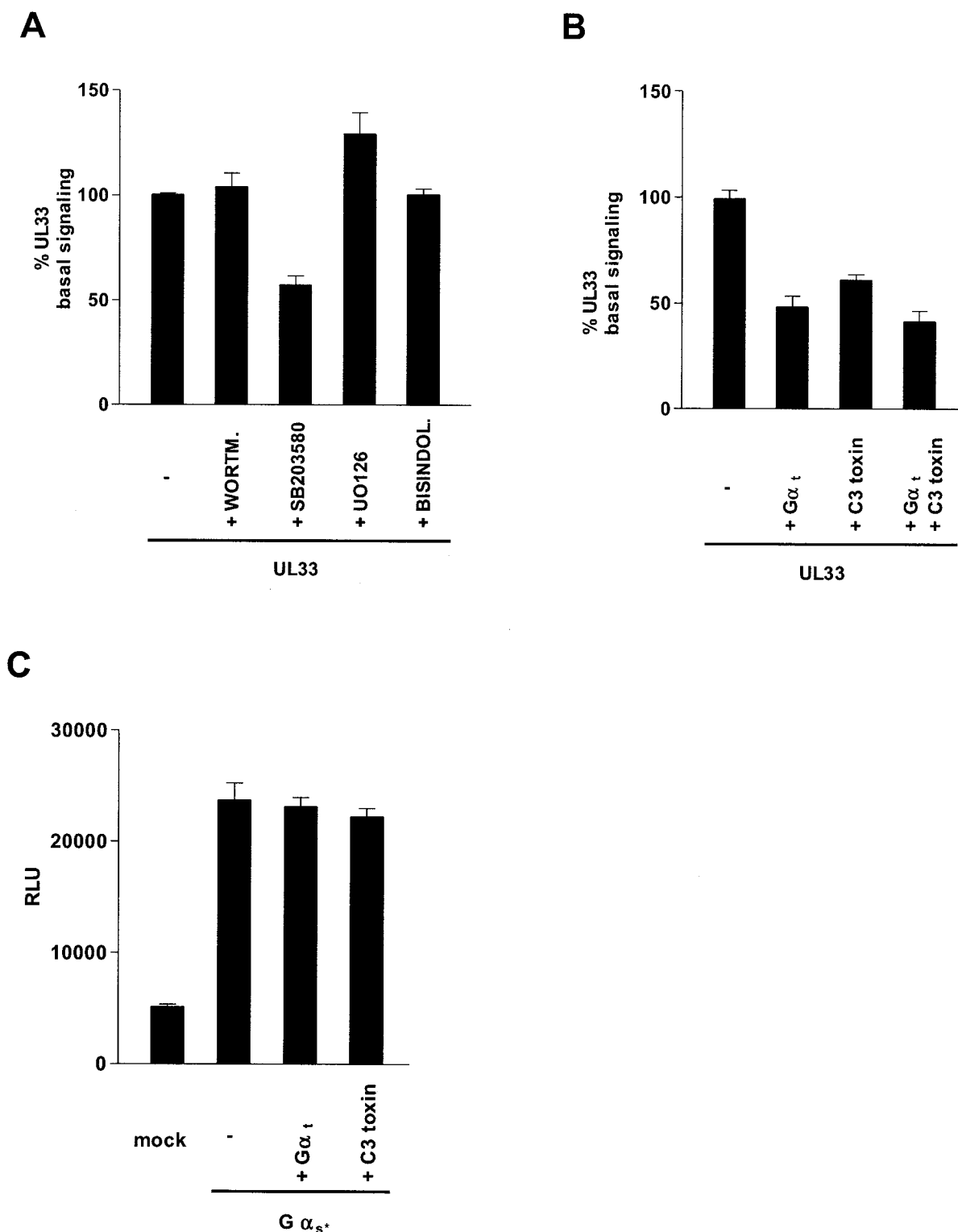
A

B

C

FIG. 7. **Additional pathways involved in the UL33-mediated CRE activation.** *A*, COS-7 cells were transfected with pTLNC-21CRE and UL33 (1 μg/10^6 cells). Cells were incubated in the presence of different specific inhibitors (purchased from Calbiochem, San Diego, CA): wortmannin (phosphatidylinositol 3-kinase inhibitor; 100 nM), SB203580 (p38 inhibitor; 2 μM), UO126 (MEK inhibitor; 1 μM), and bisindolylmaleimide (PKC inhibitor; 100 nM). One day after transfection, CRE-driven luciferase expression was measured. Data are presented as percentages of UL33-mediated response. *B*, COS-7 cells were transfected with pTLNC-21CRE and UL33 (1 μg/10^6 cells), together with combinations of cDNAs encoding Gα transducin and C3 toxin (1 μg/10^6 cells for each construct). One day after transfection, CRE-driven luciferase expression was measured. Data are presented as percentages of UL33-mediated response. *C*, COS-7 cells were transfected with pTLNC-21CRE and either pcDNA3 (mock) or Gα_s* (corresponding to Gα_s-R201E, constitutively active mutant; 1 μg/10^6 cells), together with cDNAs encoding Gα transducin or C3 toxin (1 μg/10^6 cells). One day after transfection CRE-driven luciferase expression was measured. Data are presented as relative light units (*RLUs*).

icantly different from that of R33. By contrast, replacement of the entire C-terminal tail of R33 by that of UL33 resulted in a mutant (R33-Y-UL33) that did not display activity in any of the assays used (Fig. 8, *B* and *D*). As shown above (Fig. 3*G*), this lack of activity can be attributed to the inability of R33-Y-UL33 to be expressed on the cell membrane.
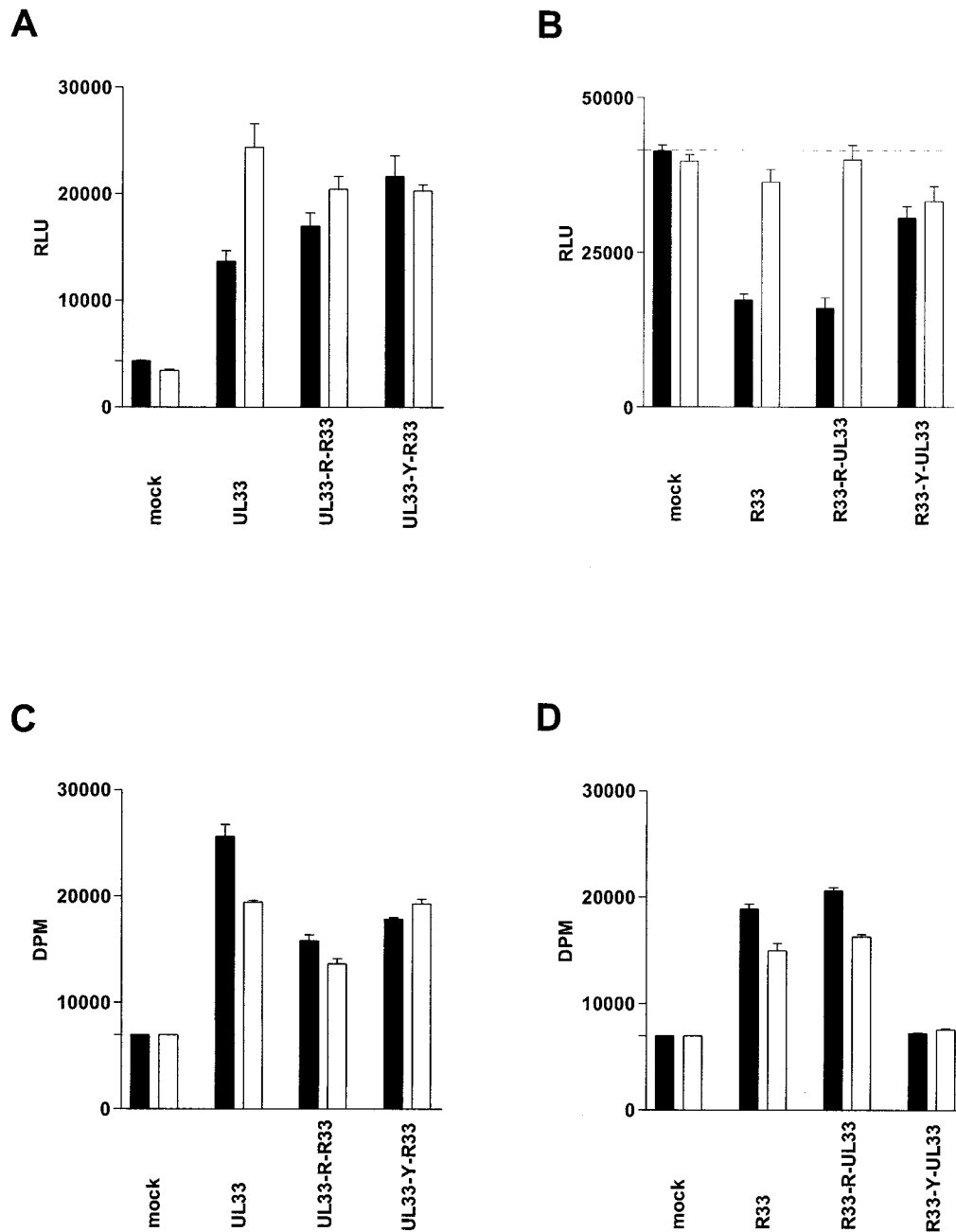
FIG. 8. **Role of the C terminus in UL33- and R33-mediated signaling.** *A* and *B*, COS-7 cells were transiently transfected with the reporter plasmid pTLNC-21CRE and cDNA encoding UL33, R33, or the different indicated chimeras (1 μg/10^6 cells; for schematic representation of chimeric proteins, see Fig. 3). Cells were incubated in the presence (*white bars*) or absence (*black bars*) of PTX (80 ng/ml). One day after transfection, CRE-driven luciferase expression was measured. For R33-WT and chimeras (*B*), cells were stimulated with forskolin for the last 6 h. *C* and *D*, COS-7 cells (1 × 10^6 cells) were transiently transfected with cDNA encoding UL33, R33, or the different indicated chimeras. Cells were incubated in the presence (*white bars*) or absence (*black bars*) of PTX (80 ng/ml). 48 h after transfection, InsP accumulation was measured.

Construction of the Deletion Mutant HCMV AD169-ΔUL33—To analyze the function of the UL33 protein in HCMV-infected cells, a *UL33*-deficient variant of HCMV AD169 (AD169-ΔUL33) was generated by mutagenesis of the AD169 genome as infectious BAC in *E. coli*.

To this end, nearly the entire coding region of UL33 was deleted (Fig. 9*A*). The recombinant virus AD169-ΔUL33 was reconstituted in fibroblasts, as described under "Material and Methods."

To confirm the deletion of *UL33* ORF in the mutant genome, Southern blot analysis was performed. Viral DNA was extracted from fibroblasts infected either with HCMV AD169 or AD169-ΔUL33, digested, separated, and hybridized with the

entire *UL33* coding region, used as probe. As can be seen in Fig. 9*B*, no signal was detected for the mutant strain, proving that the *UL33* gene has been deleted. As a positive control, the integrity of the *US28* and the *UL78* ORFs was checked with the respective probes (Fig. 9*B*). No differences could be detected in the fragment length of both regions.

Propagation of the recombinant AD169-ΔUL33 virus also revealed that the *UL33* gene product is not essential for viral growth in tissue culture, because the titers of wild-type and mutant virus stocks produced by infection of fibroblasts were identical (Fig. 9*C*).

Analysis of UL33-mediated Signaling in HCMV-infected Cells—We next investigated whether UL33 is capable of acti-
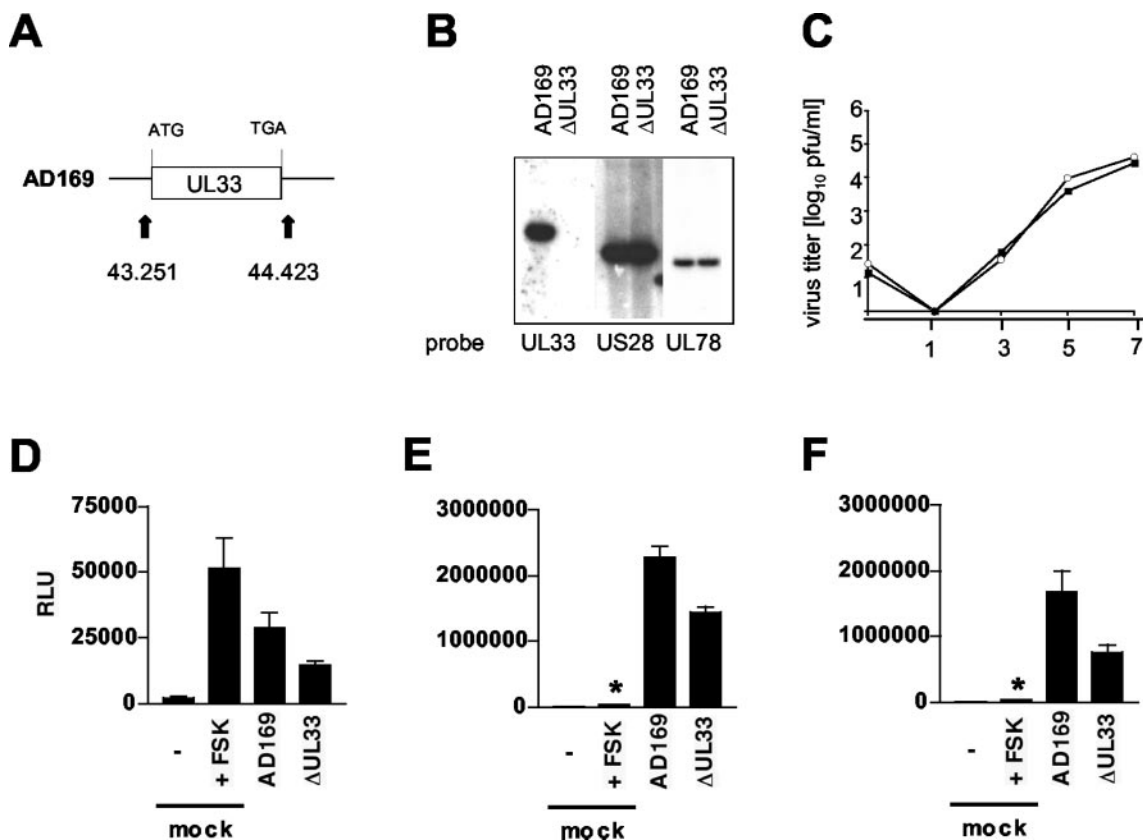
FIG. 9. **UL33 activates CRE in HCMV-infected cells.** *A*, construction of the deletion mutant HCMV AD169-ΔUL33, schematic representation of the protocol. The coding region of UL33 is shown as a *horizontal bar*. The region deleted is indicated in between *solid arrows*. The nucleotide numbering corresponding to EMBL/GenBank™ accession no. X17403 is shown. *B*, Southern blot analysis in HCMV-infected fibroblasts. Viral DNA was extracted from cells infected with either wild-type HCMV AD169 or AD169-ΔUL33. DNA was digested (with EcoRI for *UL33* and *US28*; with BamHI for *UL78*), fractionated by gel electrophoresis, and hybridized with the corresponding radiolabeled probes. *C*, virus yield kinetics. Fibroblasts were infected at an m.o.i. of 0.01 with either wild-type HCMV AD169 or AD169-ΔUL33. The *graphs* show the virus titers determined in the culture medium obtained with AD169 (*open circles*) and AD169-ΔUL33 (*closed boxes*). *D–F*, role of UL33 in HCMV-induced CRE activation. U373 cells were transiently transfected with the reporter plasmid pTLNC-21CRE and subsequently infected with wild-type HCMV AD169, AD169-ΔUL33 at an m.o.i. of 3 or mock infected. CRE-driven luciferase expression was measured 6 (*D*), 24 (*E*), and 48 h (*F*) after infection. Some samples of mock infected cells were stimulated with forskolin (indicated as *FSK*; 10 μM) for the last 6 h before read-out. Data are presented as relative light units (*RLUs*).

vating CRE in HCMV-infected cells, as suggested by results obtained in transfected COS-7 cells.

To this end, U373 cells were transiently transfected with the reporter-gene pTLNC-21CRE and subsequently infected with HCMV AD169 or AD169-ΔUL33 or mock infected. CRE activation was measured at 6, 24, and 48 h post-infection (Fig. 9, *D–F*). As internal control for transfection, some samples of mock infected cells were stimulated with forskolin (10 μM) for the last 6 h before each read-out. Forskolin-induced CRE activation was comparable at the different time points (~60,000 relative light units), suggesting that no major changes in transfection efficiency among the different time points are present.

Most interestingly, we found a marked increase of CRE activation in AD169-infected cells compared with mock infected cells (Fig. 9, *D–F*). Virus-induced CRE activation is already present at the early time point (12 ± 1-fold over mock infected cells; Fig. 9*D*) and is further increased at later time points (430 ± 50- and 318 ± 20-fold over mock infected cells at 24 and 48 h, respectively; Fig. 9, *E* and *F*). Importantly, cells infected with AD169-ΔUL33 showed a lower activation of CRE at each time point examined (Fig. 9, *D–F*): the residual CRE activation is 47 ± 3%, 62 ± 1%, and 45 ± 3% of WT-HCMV-induced signaling at 6, 24, and 48 h after infection, respectively. These data strongly imply that UL33 is at least in part responsible for virus-induced CRE activation.

DISCUSSION

Viruses have evolved various ways to alter intracellular signaling pathways (1). By means of expression of pirated GPCRs, viruses are suggested to coordinate and regulate cellular signal transduction both spatially and temporally to enhance the degree of signal specificity according to its own needs. As such, vGPCRs would significantly contribute to viral pathogenesis. Direct evidence that vGPCRs indeed contribute to pathology is available for several of these receptors. For instance, KSHV ORF74 was found to act as an oncogene (37). Moreover, transgenic expression of ORF74 induces an angioproliferative disease resembling Kaposi's sarcoma (38). Furthermore, the GPCR genes of RCMV (*R33* and *R78*) and MCMV (*M33* and *M78*) were each found to play a crucial role in the pathogenesis of viral infection (13, 14, 39, 40).

Our current data and those reported earlier by us and others (8, 9, 10, 16, 17) indicate that CMV effectively uses vGPCRs to orchestrate signaling networks within the cell during its viral life span. Previously, four genes encoding vGPCRs have been identified in the HCMV genome (*US27*, *US28*, *UL33*, and *UL78*) (4). Although a recent study has suggested that the HCMV genome contains an additional 11 genes that putatively encode proteins possessing 7 transmembrane domains (5), these genes seem to lack other sequences characteristic of the family of GPCR genes. Of the four putative HCMV genes, only

US28 and *UL33* have hitherto been demonstrated to encode functional GPCRs (Refs. 8 and 17, and this study). Previously, US28 has been shown to constitutively activate a variety of signal transduction cascades, including PLC (8), MAPK pathways (41), and various transcription factors (8, 17). Moreover, we and others have recently shown that also in HCMV-infected fibroblasts US28 constitutively activates PLC (9, 10), further emphasizing the physiological relevance of the constitutive signaling of US28 after viral infection. Here, we show that another HCMV-encoded receptor, UL33, displays constitutive signaling in transfected as well as in HCMV-infected cells.

Until now, the structure of the *UL33* cDNA was predicted on the basis of sequence analyses as well as the finding of an intron near the 5′ end of the *UL33* open reading frame. In this study, we have shown that UL33 predominantly encodes a spliced transcript of which the 5′ terminus is located 55 bp upstream of the start codon. No evidence was found for the existence of an unspliced UL33 transcript, which could potentially encode a shorter version of UL33 such as the one used in this study, *i.e.* UL33(s). The observed lack of membrane expression and signaling of UL33(s) indicates that it is indeed unlikely that this hypothetical UL33 gene product is relevant in HCMV infection.

As reported previously (10, 16, 17, 42), our present results with UL33 indicate that a high level of constitutive activity appears to be an important property of vGPCRs. Viruses might exploit this inherent GPCR property to modulate homeostasis of infected cells. UL33 is, like R33, M33, and US28, positively coupled to PLC, generating an increase in inositol phosphate production. For both UL33 and R33, activation of PLC is mediated not only by $G_{q/11}$ proteins, but also partially by $G_{i/o}$ proteins (Fig. 10*A*). $G\alpha_{q/11}$ and $G\beta\gamma$ subunits from $G_{i/o}$ appear to be the most likely components activating PLC. UL33 and its RCMV counterpart R33 differ, however, in their ability to modulate activation of CRE transcription. R33 constitutively inhibits signaling to CRE, measured as a reduction of forskolin-induced signaling. Inhibition of CRE-driven transcription by R33 is entirely $G_{i/o}$-mediated (Fig. 10*B*), preferably through G_{i1} and G_{i3} (Fig. 6*A*). By contrast, UL33 appears to possess a broader range of G protein coupling. Although UL33 interacts with G proteins of the $\alpha_{i/o}$ class (most likely G_{i1} and G_{i3}), additional signal transduction routes play a more prominent role with respect to CRE activation; as a result, the overall effect of UL33 signaling is a transcriptional activation of CRE (Fig. 10*B*). CREB is regulated by a concerted action of various signaling kinases such as PKA, PKC, MAPKs, including p44/p42 and p38 (30), many of which are up-regulated early after CMV infection (41). UL33-mediated transcriptional activation of CRE appears to be mediated by coupling to $G\alpha_s$, on one hand, and signaling through Rho and p38, via $G\beta\gamma$, on the other. Because co-expression of $G\alpha_t$ and C3 exoenzyme does not result in a further decrease in UL33-mediated signaling to CRE, it is likely that signaling pathways converge. Rho is known to activate p38 via MKK3/6 (36), leading to phosphorylation of CREB, possibly via MSK-1 (43).

Interestingly, we noticed that co-expression of $G\alpha_q$ reduced UL33-mediated CRE transcription. Apparently, this effect was not due to a direct negative regulation of CRE, as shown by data obtained either with the constitutively active $G\alpha_{11}*$ subunit or in the presence of PKC activator PMA. As an alternative explanation, we suggest that overexpression of $G\alpha_q$ is actually scavenging the receptor from coupling to G_s subunits, resulting in a reduction of CRE activation. In line with this hypothesis, we found that overexpression of $G\alpha_s$ strongly reduced UL33-mediated InsP accumulation (data not shown). Similar results were previously shown for the α_2-adrenorecep-
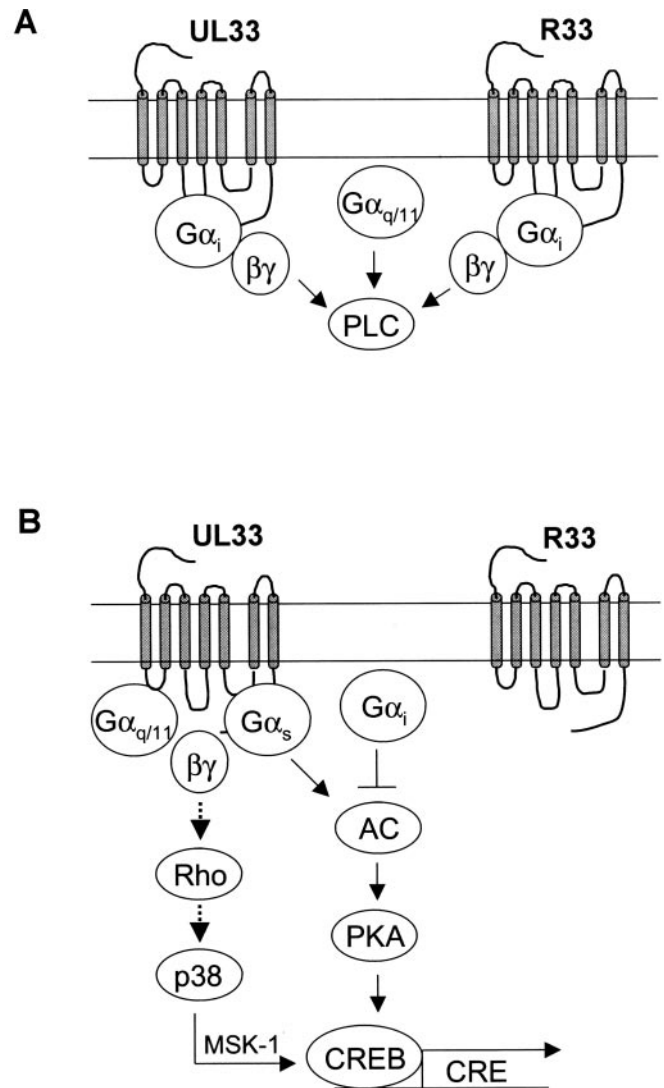

FIG. 10. **Proposed model of UL33 and R33-mediated signaling.** *A*, UL33 and R33 activate PLC via coupling to $G\alpha_{q/11}$ subunits and via $\beta\gamma$ subunits released from $\alpha_{i/o}$ proteins. *B*, UL33 and R33 differentially regulate CRE-mediated transcription. Whereas both receptors show a $G\alpha_{i/o}$-mediated inhibition of cAMP levels, UL33 also couples to $G\alpha_s$, which activates adenylyl cyclase (*AC*). Additionally, $\beta\gamma$ subunits are partly responsible for UL33-mediated CRE activation. We suggest that this pathway involves the activation of Rho/p38, finally leading to the phosphorylation of CREB.

tor, which can couple to both $G\alpha_i$ and $G\alpha_s$ subunits. Co-expression of either $G\alpha_i$ or $G\alpha_s$ subunits resulted in an agonist-mediated inhibition or increase of cAMP levels, respectively (44). The interaction with an overexpressed G protein excludes interaction with others; therefore, the availability of G proteins of different classes can significantly alter the signaling response for broadly coupled receptors.

The apparent divergent and opposite signaling properties of the UL33 and R33 receptors prompted us to investigate the differences between these proteins in more detail. Sequence comparison indicated that the observed differences in activity might be due to their divergent C-terminal tails. The predicted amino acid sequence of UL33 has a relatively long C-terminal tail in comparison with R33. Remarkably, R33 contains a unique stretch of 11 consecutive Pro residues (polyproline stretch) near the C terminus. Although polyproline motifs have previously been shown to mediate binding to a variety of conserved protein domains, such as Src homology 3 (SH3) and WW domains (45), the role of this motif in the function of R33 is yet

unknown. To investigate the role of the C-terminal tails in the differential signaling profiles of UL33 and R33, we generated UL33/R33 chimeras. Interestingly, the study of these chimeras showed that the C-terminal tail of UL33 appears to be the determinant for signaling of UL33 via $G_{i/o}$. Exchanging (part of) the C terminus of UL33 for the C terminus of R33, resulted in a loss of $G_{i/o}$ coupling, as observed in both the InsP accumulation assay and CRE reporter gene assay.

Conversely, exchange of the C terminus of R33 for that of UL33, did not significantly alter R33-mediated signaling, suggesting that sequences other than the C terminus are important for coupling of R33 to $G_{i/o}$. It is interesting to note that R33 contains a basic motif (including $^{314}KRF^{316}$) that has recently been shown to play a crucial role in proper receptor expression of CCR5 (46). It was found that substitution of the C-terminal tail of CCR5, which comprises this basic motif, for that of CXCR4, which lacks it, resulted in a mutant that was defective in trafficking to the cell surface, whereas the CXCR4 chimera that exchanged the C terminus for that of CCR5 displayed a normal, cell surface expression pattern. In analogy, the lack of the basic motif from chimera R33-Y-UL33 may explain the inability of this protein to be expressed properly on the cell surface and, thus, its inactivity in any of the signaling assays. Additionally, the UL33 tail contains an RXR motif ($^{316}RMR^{318}$), known to be implicated in protein retention in the endoplasmic reticulum (52). It is possible that this motif is masked in the UL33 receptor, but is exposed within chimera R33-Y-UL33, thereby conferring endoplasmic reticulum localization.

To date, UL33 homologs from rodent CMVs, R33 and M33, remain orphan receptors, as chemokines, which either modulate the activity of, or bind to, these receptors, have not yet been found (16, 17). Similarly, the CC chemokines RANTES (regulated on activation normal T cell expressed and secreted), and MIP-1α did not modulate UL33 constitutive activity nor showed any binding to this receptor (data not shown). The recent identification of a small non-peptidergic inverse agonist for US28 by its modulating effect on US28-mediated constitutive signaling (9), demonstrates that the UL33-mediated signaling assays described in this study may be suitable screening systems for the identification of ligands acting at UL33. The availability of such a ligand would be of help in elucidating the role of UL33 in HCMV infection.

Little is known about the mechanisms underlying the pathogenesis of human cytomegalovirus. It is known that, following CMV infection, effector responses such as inositol lipid hydrolysis, kinase activation, and arachidonic acid metabolism are increased within the host cell and are required to direct and control early viral gene expression and DNA replication (47). Here we show that HCMV also induces a strong activation of CRE, at early and late times post infection. In this regard, it is important to note that the HCMV major immediate-early promoter contains four consensus CRE sites (48, 49). Because the immediate-early promoter of HCMV constitutes a primary genetic switch, essential for the progression of viral infection and reactivation, regulation of CRE activation during the infectious course might be of (patho)physiological importance. Importantly, data obtained with the deletion mutant virus AD169-ΔUL33 strongly indicate that UL33 is involved in virus-induced CRE activation. At all time points, ΔUL33 induces approximately only half the response of WT virus. These results cannot be ascribed to an impaired infectivity of the deletion mutant virus, because we have shown that viral growth kinetics are essentially the same for WT and ΔUL33-HCMV (Fig. 9C). These findings confirm the UL33-mediated CRE activation in a physiologically relevant model system. Infection of cells with HCMV offers a significant model for the pharmaco-logical study of UL33, because in this condition UL33 expression is regulated by the virus and its constitutive signaling is not a potential artifact due to overexpression. Interestingly, UL33 contribution to CRE activation was already present at early time post infection. Because UL33 is mainly transcribed at late times of infection (13), it is likely that UL33 expression on the virion envelope, as described previously (12, 50), activates signal transduction pathways immediately upon infection, after fusion of the viral envelope with the cell membrane. Comparison of CRE activation in cells infected with ΔUL33 CMV or mock infected also indicates that UL33 is not the only player involved in HCMV-induced CRE activation. It is suggestive to propose US28 as a candidate for the residual CRE activation, because it was shown that this receptor can also activate CRE in transiently transfected COS-7 cells, similarly to UL33 (17). We are currently investigating in more detail the signaling pathways engaged by HCMV in CRE activation. Interestingly, it was recently shown that HCMV infection induces p38 phosphorylation (51). The role of UL33 and US28 in HCMV-induced p38 activation and its possible link to CRE activation, as suggested by results obtained in COS-7 cells, will be further examined.

In conclusion, it is apparent from these and earlier studies that CMV-encoded receptors regulate cellular signaling via the constitutive activation of a range of G proteins. In this study, we show that UL33 constitutively modulates several pathways via promiscuous activation of G proteins of different classes. Initial experiments performed with HCMV-infected cells suggest that the signaling properties of UL33 are of physiological relevance and that HCMV may effectively use UL33 and US28 to orchestrate multiple signaling networks within infected cells.

REFERENCES

1. Murphy, P. M. (2001) *Nat. Immunol.* **2,** 116–122
2. Rosenkilde, M. M., Waldhoer, M., Luttichau, H. R., and Schwartz, T. W. (2001) *Oncogene* **20,** 1582–1593
3. Sweet, C. (1990) in *Topley and Wilson's Principles of Bacteriology*, (Collier, L. S., and Timbury, M. C., eds) Vol. 4, 8th Ed., pp. 105–130, Edward Arnold, London
4. Chee, M. S., Satchwell, S. C., Preddie, E., Weston, K. M., and Barrell, B. G. (1990) *Nature* **344,** 774–777
5. Rigoutsos, I., Novotny, J., Huynh, T., Chin-Bow, S. T., Parida, L., Platt, D., Coleman, D., and Shenk, T. (2003) *J. Virol.* **77,** 4326–4344
6. Kuhn, D. E., Beall, C. J., and Kolattukudy, P. E. (1995) *Biochem. Biophys. Res. Commun.* **211,** 325–330
7. Kledal, T. N., Rosenkilde, M. M., and Schwartz, T. W. (1998) *FEBS Lett.* **441,** 209–214
8. Casarosa, P., Bakker, R. A., Verzijl, D., Navis, M., Timmerman, H., Leurs, R., and Smit, M. J. (2001) *J. Biol. Chem.* **276,** 1133–1137
9. Casarosa, P., Menge, W. M., Minisini, R., Otto, C., van Heteren, J., Jongejan, A., Timmerman, H., Moepps, B., Kirchhoff, F., Mertens, T., Smit, M. J., and Leurs, R. (2003) *J. Biol. Chem.* **278,** 5172–5178
10. Minisini, R., Tulone, C., Luske, A., Michel, D., Mertens, T., Gierschik, P., and Moepps, B. (2003) *J. Virol.* **77,** 4489–4501
11. Vink, C., Smit, M. J., Leurs, R., and Bruggeman, C. A. (2001) *J. Clin. Virol.* **23,** 43–55
12. Margulies, B. J., Browne, H., and Gibson, W. (1996) *Virology* **225,** 111–125
13. Davis-Poynter, N. J., Lynch, D. M., Vally, H., Shellam, G. R., Rawlinson, W. D., Barrell, B. G., and Farrell, H. E. (1997) *J. Virol.* **71,** 1521–1529
14. Beisser, P. S., Vink, C., Van Dam, J. G., Grauls, G., Vanherle, S. J., and Bruggeman, C. A. (1998) *J. Virol.* **72,** 2352–2363
15. Isegawa, Y., Ping, Z., Nakano, K., Sugimoto, N., and Yamanishi, K. (1998) *J. Virol.* **72,** 6104–6112
16. Gruijthuijsen, Y. K., Casarosa, P., Kaptein, S. J., Broers, J. L., Leurs, R., Bruggeman, C. A., Smit, M. J., and Vink, C. (2002) *J. Virol.* **76,** 1328–1338
17. Waldhoer, M., Kledal, T. N., Farrell, H., and Schwartz, T. W. (2002) *J. Virol.* **76,** 8161–8168
18. Beisser, P. S., Laurent, L., Virelizier, J. L., and Michelson, S. (2001) *J. Virol.* **75,** 5949–5957
19. Goossens, V. J., Blok, M. J., Christiaans, M. H., Sillekens, P., Middeldorp, J. M., and Bruggeman, C. A. (2000) *Transplant Proc.* **32,** 155–158
20. Altschul, S. F., Gish, W., Miller, W., Myers, E. W., and Lipman, D. J. (1990) *J.*

Mol. Biol. **215,** 403–410
21. Wagner, M., and Koszinowski, U. H. (2004) in *Methods in Molecular Biology* (Zhao, S., ed) Vol. 23, Humana Press, Totowa, NJ, in press
22. Wagner, M., Ruzsics, Z., and Koszinowski, U. H. (2002) *Trends Microbiol.* **10,** 318–324
23. Atalay, R., Zimmermann, A., Wagner, M., Borst, E., Benz, C., Messerle, M., and Hengel, H. (2002) *J. Virol.* **76,** 8596–8608
24. Sambrook, J., and Russell, D. W. (2001) *Molecular Cloning: A Laboratory Manual*, Cold Spring Harbor Laboratory, Cold Spring Harbor, NY
25. Wagner, M., Michel, D., Schaarschmidt, P., Vaida, B., Jonjic, S., Messerle, M., Mertens, T., and Koszinowski, U. (2000) *J. Virol.* **74,** 10729–10736
26. Lee, S. B., Shin, S. H., Hepler, J. R., Gilman, A. G., and Rhee, S. G. (1993) *J. Biol. Chem.* **268,** 25952–25957
27. Diviani, D., Lattion, A. L., Larbi, N., Kunapuli, P., Pronin, A., Benovic, J. L., and Cotecchia, S. (1996) *J. Biol. Chem.* **271,** 5049–5058
28. Alewijnse, A. E., Smit, M. J., Rodriguez Pena, M. S., Verzijl, D., Timmerman, H., and Leurs, R. (1997) *FEBS Lett.* **419,** 171–174
29. Wise, A., Sheehan, M., Rees, S., Lee, M., and Milligan, G. (1999) *Biochemistry* **38,** 2272–2278
30. Shaywitz, A. J., and Greenberg, M. E. (1999) *Annu. Rev. Biochem.* **68,** 821–861
31. Smit, M. J., Verzijl, D., Casarosa, P., Navis, M., Timmerman, H., and Leurs, R. (2002) *J. Virol.* **76,** 1744–1752
32. Lopez-Ilasaca, M. (1998) *Biochem. Pharmacol.* **56,** 269–277
33. Aznar, S., and Lacal, J. C. (2001) *Cancer Lett.* **165,** 1–10
34. Sekine, A., Fujiwara, M., and Narumiya, S. (1989) *J. Biol. Chem.* **264,** 8602–8605
35. Sah, V. P., Seasholtz, T. M., Sagi, S. A., and Brown, J. H. (2000) *Annu. Rev. Pharmacol. Toxicol.* **40,** 459–489
36. Yamauchi, J., Tsujimoto, G., Kaziro, Y., and Itoh, H. (2001) *J. Biol. Chem.* **276,** 23362–23372
37. Bais, C., Santomasso, B., Coso, O., Arvanitakis, L., Raaka, E. G., Gutkind, J. S., Asch, A. S., Cesarman, E., Gershengorn, M. C., Mesri, E. A., and Gerhengorn, M. C. (1998) *Nature* **391,** 86–89
38. Yang, T. Y., Chen, S. C., Leach, M. W., Manfra, D., Homey, B., Wiekowski, M., Sullivan, L., Jenh, C. H., Narula, S. K., Chensue, S. W., and Lira, S. A. (2000) *J. Exp. Med.* **191,** 445–454
39. Beisser, P. S., Grauls, G., Bruggeman, C. A., and Vink, C. (1999) *J. Virol.* **73,** 7218–7230
40. Oliveira, S. A., and Shenk, T. E. (2001) *Proc. Natl. Acad. Sci. U. S. A.* **98,** 3237–3242
41. Billstrom, M. A., Johnson, G. L., Avdi, N. J., and Worthen, G. S. (1998) *J. Virol.* **72,** 5535–5544
42. Arvanitakis, L., Geras-Raaka, E., Varma, A., Gershengorn, M. C., and Cesarman, E. (1997) *Nature* **385,** 347–350
43. De Cesare, D., Fimia, G. M., and Sassone-Corsi, P. (1999) *Trends Biochem. Sci.* **24,** 281–285
44. Nasman, J., Kukkonen, J. P., Ammoun, S., and Akerman, K. E. (2001) *Biochem. Pharmacol.* **62,** 913–922
45. Pawson, T., and Scott, J. D. (1997) *Science* **278,** 2075–2080
46. Venkatesan, S., Petrovic, A., Locati, M., Kim, Y. O., Weissman, D., and Murphy, P. M. (2001) *J. Biol. Chem.* **276,** 40133–40145
47. Albrecht, T., Boldogh, I., Fons, M., AbuBakar, S., and Deng, C. Z. (1990) *Intervirology* **31,** 68–75
48. Hunninghake, G. W., Monick, M. M., Liu, B., and Stinski, M. F. (1989) *J. Virol.* **63,** 3026–3033
49. Sun, B., Harrowe, G., Reinhard, C., Yoshihara, C., Chu, K., and Zhuo, S. (2001) *J. Cell. Biochem.* **83,** 563–573
50. Fraile-Ramos, A., Pelchen-Matthews, A., Kledal, T. N., Browne, H., Schwartz, T. W., and Marsh, M. (2002) *Traffic* **3,** 218–232
51. Johnson, R. A., Huong, S. M., and Huang, E. S. (2000) *J. Virol.* **74,** 1158–1167
52. Shikano, S., and Li, M. (2003) *Proc. Natl. Acad. Sci. U. S. A.* **100,** 5783–5788